BMC Cardiovascular Disorders

RESEARCH

Open Access

Empagliflozin ameliorates RSL3-induced ferroptosis in vascular endothelial cells via the NRF2/HO-1 pathway

ZiLin Wang[1†], SiMiao Liu[1†], JiaHao Shi[1], Di Chen[1], ShaoLin Li[1], ShengQin Yu[1], SiXu Liu[1], KaiJing Yang[1], Wan Zhang[1], Xue Gao[1] and ShuYing Zhang[1*]

Abstract

Endothelial cell dysfunction is a fundamental injury of atherosclerosis cardiovascular disease (ASCVD), closely linked to ferroptosis, which is a novel type of cell death induced by iron-dependent lipid peroxidation. Several clinical trials have suggested that empagliflozin, a selective inhibitor of sodium glucose co-transporter 2, reduces the risk of hospitalization for heart failure and cardiovascular death in patients with type 2 diabetes. However, little is known about the mechanism of EMPA in endothelial cell ferroptosis in ASCVD. The aim of the present study was to evaluate the potential mechanism of EMPA against ferroptosis induced by RAS-selective lethal 3 (RSL3) in endothelial cells.

EA.hy926 human umbilical vein endothelial cells were cultured in vitro and were divided into four groups: The Control, RSL3, RSL3 + low-concentration EMPA intervention and RSL3 + high-concentration EMPA intervention groups. Iron-dependent lipid peroxidation was assessed by detecting the fluorescence intensity of ferrous ion (Fe^{2+}), lipid reactive oxygen species (ROS) and content of malondialdehyde (MDA). The expression of ferroptosis-related genes was assessed by RT-qPCR and western blotting. siRNA nuclear factor erythroid 2-related factor 2 (NRF2) was transfected into EA.hy926 cells to measure the expression of target genes.

It was demonstrated that the level of MDA, Fe^{2+} and lipid ROS was higher in the RSL3-treated group compared with the EMPA intervention group, while EMPA markedly mitigated that effect. In addition, EMPA can reverse the RSL3-induced low expression of glutathione peroxidase 4 (GPX4) and high expression of ACSL4 in endothelial cells, as evidenced by the upregulation of nuclear factor transcription factor nuclear factor, erythroid 2 (NFE2)-related factor 2 and heme oxygenase-1 expression, while siNRF2 transfection impaired the antiferroptosis effect of EMPA. The present study indicated that EMPA may inhibit RSL3-induced ferroptosis in endothelial cells by activating the NRF2/heme oxygenase 1 gene pathway.

Keywords Empagliflozin, Ferroptosis, Endothelial cell injury, NRF2, HO-1

†ZiLin Wang and SiMiao Liu are first authors and contribute equally.

*Correspondence:
ShuYing Zhang
zhangshuying2024@163.com
[1]Affiliated Zhongshan Hospital of Dalian university, Dalian 116001, China

Introduction

Atherosclerotic cardiovascular disease (ASCVD) is strongly associated with pathological changes in endothelial cells. Due to their dysfunction, endothelial cells are unable to effectively regulate blood flow and pressure, secreting a variety of adhesion factors that attract neutrophils and monocytes to form atheromatous areas in the inner wall of the blood vessel, which eventually results in lumen reduction, blockage and even plaque rupture [1, 2]. Due to a variety of factors, the treatment of endothelial cell injury are not yet clear.

Ferroptosis is a type of regulated cell death mediated by iron-dependent lipid peroxidation, and its pathogenesis is associated with iron metabolism, lipid and glutathione (GSH) metabolism. Acyl-CoA synthetase long chain family member 4 (ACSL4) is a key enzyme in fatty acid metabolism that promotes the metabolic esterification of polyunsaturated fatty acids to phosphatidyl ethanolamine [3]. These modified phospholipids undergo iron-mediated Fenton reactions to generate lipid hydroperoxides, thereby compromising membrane integrity. Concurrently, impaired recombinant solute carrier family 7, Member 11 (SLC7A11) function reduces glutathione biosynthesis, while glutathione peroxidase 4 (GPX4) deficiency diminishes antioxidant defenses. This dual impairment of lipid peroxide elimination and redox homeostasis constitutes the core mechanism driving ferroptosis [4, 5]. Recent studies have also shown that increased iron stores lead to vascular endothelial cell dysfunction in apolipoprotein E knockout mice or patients with coronary artery disease [6, 7]. Hence, protecting endothelial cells from ferroptosis plays a vital role in the improvement of ASCVD progression.

As a new hypoglycemic agent, sodium-dependent glucose transporter protein 2 inhibitors (SGLT2i) have attracted increasing attention for its cardiovascular effects [8]. In myocardial ischaemia-reperfusion, Empagliflozin (EMPA) protects the homeostasis of cardiac microvascular endothelial cells by activating the mitochondrial autophagy pathway and repressing mitochondrial fission [9, 10]. It has also been shown that SGLT2i protects endothelial cells by increasing their nitric oxide utilization [11]. Furthermore, EMPA inhibits stretch-induced nicotinamide adenine dinucleotide phosphate oxidase (NOX) activation and reactive oxygen species (ROS) generation in endothelial cells by preventing protein kinase C (PKC) activation [12]. The above studies have suggested that EMPA plays an important role in endothelial cell protection thus improving ASCVD. However, whether EMPA can protect endothelial cells from ferroptosis has not yet been completely elucidated.

The multifunctional regulatory nuclear factor erythroid 2-related factor 2 (NRF2) is a cytoprotective factor that can regulate the expression of encoded antioxidant and anti-inflammatory factors, and may be involved in the regulation of oxidative stress in cardiovascular disease [13]. It has now been shown that genes involved in ferroptosis are regulated by the NRF2/heme oxygenase 1 gene (HO-1) pathway [14]. Therefore, we hypothesized that EMPA may inhibit iron-dependent lipid peroxidation in endothelial cells by activating the NRF2/HO-1 pathway.

Materials and methods

Cell culture

The Human umbilical vein endothelial EA.hy926 cell lines were kindly provided by Cell Bank, Chinese Academy of Sciences, supplemented with DMEM/F12 complete medium(Gibco, Thermo Fisher) that containing 10% fetal bovine serum (Newzerum FBS, New Zealand) and 1% Penicillin-streptomycin mixture (keygen BIO, China) and incubated under 37℃, and 5% CO_2 standard condition until density of cells reached to 80-90% confluence. Cells divided into four groups: Control group, RSL3 group, RSL3 + low-concentration EMPA intervention group, and RSL3 + high-concentration EMPA intervention group. The stock solution of EMPA (HY-15409, MedChem Express) or RSL3 (HY-100218 A, MedChem Express) was prepared in DMSO and subsequently diluted with culture medium containing 2% FBS.

Cell viability

To screen for the optimal concentration of RSL3 and EMPA. Drug-activated cell viability was detected by CCK8 reagent (APE x BIO, USA). The density of cell was adjusted to 1×10^5/mL and then 100 μL of cell suspension was added to each well of 96-well plates. The cells with 80-90% confluence was separately exposed to the diluted concentration of RSL3 solution (0.5, 1, 1.5, 2, and 3.5 μM) for 12–24 h. EMPA (0.25, 0.5 and 1 μM) and both drugs combined for 24 h. Finally, cells were incubated with 110 μL of medium contains 10% CCK-8 for each well and placed in a constant temperature 37℃ for 1–1.5 h, taking care to avoid light throughout. The OD values of 96-well plates were measured at 450 nm using a microplate reader (Thermo Fisher).

Detection of lipid peroxidation

BODIPYTM581/591C11 (D3861, Thermo Fisher) is a lipid peroxidation sensor, which can be detected by flow cytometry (OLYMPUS) and fluorescence microscope (OLYMPUS). The EA.hy926 cells were stained with 10 μM BODIPYTM581/591C11 dilution and incubated in a dark environment. After waiting for 30 min, the cells were then washed with phosphate-buffered saline (PBS) 2–3 times in order to wash away dyestuffs.

Cells were digested with 0.25% trypsin-EDTA and centrifuged at 900 × g for 5 min at 4 °C using a refrigerated

centrifuge. After supernatant removal, the pellet was washed twice with PBS through sequential resuspension and centrifugation at 900 × g for 3 min. The fluorescence intensity was quantified with negative controls setting photomultiplier tube voltages. Cellular lipid peroxidation levels were determined by gating intact cell populations and analyzing median fluorescence intensity (MFI) using FlowJo™ software [15].

To assess the inner lipid peroxidation of the EA.hy926 cells through qualitative method, the cells were continually stained with DAPI (P0131, Beyotime Biotechnology) to mark nucleus and observed by fluorescence microscope in a dark enviroment throughout. Finally, analyzed by ImageJ.

Determination of intracellular Fe^{2+} and MDA

FerroOrange (F314, DOJINDO) was used to detect intracellular Fe^{2+} sensitively. Firstly, the EA.hy926 cells were washed with HBSS balanced salt solution (C0219, Beyotime Biotechnology) three times, then stained with appropriate amount of DAPI for 3–5 min and aspirated out, and washed with HBSS balanced solution for 2–3 times. Secondly, stained with working solution concentration of 1 μM of FerroOrange for 30 min in 24-well plate. After that, the plate was placed in the incubator at 37℃ for 30 min. Images were captured by fluorescence microscope, and the whole process was avoided from light. The images were taken using a fluorescence microscope, protected from light throughout the process, and quantitatively analyzed by ImageJ software.

Malondialdehyde assay kit (A003-1-2, Jiancheng, Nanjing, China) was used to measure MDA level in cell lysate. The wavelength used for measurement was 532 nm, and then MDA concentration was calculated by creating a standard curve and normalizing it to the protein content.

Small interfering transfection

The sequence of siRNA-NRF2 (GenePharma, China; F:5'-CCAGAACACU-CAGUGGAAUTT-3' and R:5'-AUUCCACUGAGUGUUCUGGTT-3') was used t-o knock down the expression of NRF2. The siRNA complexes were prepared by mixing 100 pmol siRNA with 5 μL GP-transfection-mate reagent (GenePharm-a, China) at 1:1 (V/V) ratio in serum-free medium After 15 min incubation at room temperature, the complexes were added to the cells for 4–6 h and subsequently replaced by complete medium. The EA.hy926 cells were divided into four groups: si-NC, si-NRF2, si-NC + RSL3/EMPA, si-NRF2 + RSL3/EMPA.

Quantitative real-time-PCR

The total RNA was isolated from EA.hy926 cells using Trizol reagent (Themor Fisher, USA) and reversely transcribed into cDNA according to kit's manufacturer's instruction (RR047A, Takara, Japan). Gene expression level were quantified by StepOnePlus real-time PCR system (Thermor Fish, USA). The primers sequence was as followed: GPX4: (F)5'-CCAGTGAGGCAAGACCGAAG T-3' (R)5'-TTGGGTTGGATCTTCATCCAC-3'; ACSL4: (F)5'-CCAGTGAGGCAAGACCGAAGT-3' (R)5'-TTG GGTTGGATCTTCATCCAC-3'; SLC7A11: (F)5'-CCC TGAACTTGCGATCAAGCT-3' (R)5'-GCTCCAGCTG ACACTCATG CT-3'; and housekeeping gene GAPDH: (F)5'-GCCAAGGTCATCCATGACAAC-3' (R)CAGCGT CAAAGGTGGAGGAGT. The relative amount of mRNA was determined using $2^{-\Delta\Delta Ct}$ method and normalized to the level of GAPDH.

Western blot

The EA.hy926 cells were rinsed twice with ice-cold PBS. After removing PBS, cells in the 6-well plate were lysed with 100 μL/well of ice-cold RIPA lysis buffer (P0013B, Beyotime Biotechonogy) supplemented with 1 mM phenylmethylsulfonyl fluoride (PMSF, ST506, Beyotime Biotechonogy). Then the cell lysate were scraped down with a cell scraper, transferred to 1.5 mL microcentrifuge tubes and homogenized through a 22-gauge needle for 10–15 cycles on ice. Centrifugated at 3000 rpm/min and 4 °C for 15 min, the protein was detected with BCA protein colorimetric assay kit (Elaboscience, Wuhan, China). The Protein of all samples were then electrophoresed in 12.5% SDS-PAGE gel, transferred to PVDF, and blocked in 5% BSA for 1 h at room temperature. The PVDF were incubated with the primary antibody of anti-GPX4 (1:5000, Abcam), anti-ACSL4 (1:3000, Proteintech), anti-SLC7A11 (1:2000, Abcam), anti-NRF2 (1:3000, Proteintech), anti-HO-1 (1:3000, Proteintech), anti-GAPDH (1:50000, Proteintech) or anti-βactin (1:3000, Abcam) at 4℃ overnight. The combined primary antibody were washed with 1 × TBST (Servicebio, Wuhan, China) three times, and incubated with HRP-conjugated goat anti-mouse IgG (1:50000, Proteintech) or HRP-conjugated goat anti-rabbit IgG (1:50000, Proteintech) for 2 h at room temperature, and then were washed three times with 1 × TBST for 10 min each time. After the ECL luminescent solution (Tano, Shanghai, China) was prepared, the PVDF was evenly dropped on protein side to be exposed under Gel Imager (BIO RAD, USA). Using ImageJ software to analyze the grey value of the immunoreactive bands.

Statistical analysis

The values of each group were expressed as mean ± standard deviation. Statistical data were analyzed using GraphPad Prism, and one-way ANOVA was used to compare the differences between the groups, with P-value less than 0.05 being considered a statistically significant difference.

Results

EMPA reduces RSL3-induced cytotoxicity in EA.hy926 cells. The results of CCK-8 showed that the viability of the EA.hy926 cells gradually decreased with the increasing RSL3 concentration and duration of the drug effect. Compared with the control group, 2–3 μM RSL3 was found to lower the cell survival rate by 50%, which can be considered as the inducing concentration (Fig. 1A). Hence, in the subsequent experiment, RSL3 (3 μM) was combined with EMPA (0.25, 0.5 and 1 μM) to treat cells for 24 h. The CCK-8 results suggested that the viability and morphology of EA.hy926 cells were gradually restored as the concentration of EMPA intervention increased compared with the RSL3 group (Fig. 1B and C). The above results suggested that EMPA has a potential benefit to protect the EA.hy926 cells from RSL3 toxicity.

EMPA reduces iron dependent lipid peroxidation reaction. The RSL3-linked content of iron, lipid peroxidation and MDA induced the dysfunction of the EA.hy926 cells, as determined by quantitative or qualitative methods. Fluorogram results showed that the fluorescence intensity of intracellular iron was markedly increased following RSL3 treatment, as compared with the control group, while the intracellular fluorescence intensity was markedly decreased following the addition of the EMPA intervention compared with the RSL3 group (Fig. 2A). In addition, the fluorescence intensity of intracellular lipid peroxidation was increased in RSL3-treated cells compared with the control group, and fluorescence intensity was weakened by the addition of EMPA intervention compared with the RSL3 group (Fig. 2B). Furthermore, flow cytograms showed that the oxidative intensity was increased in the RSL3 group compared with the control group, while the oxidative intensity was significantly weakened in the EMPA intervention group compared with the RSL3 group (Fig. 2C). MDA is one of the products of lipid peroxidation. The results showed that the intracellular MDA content was markedly higher in the RSL3 group compared with the control group. Following EMPA treatment, the MDA content was lower compared with the RSL3 group in a concentration-dependent manner (Fig. 2D). The above results suggested that EMPA as

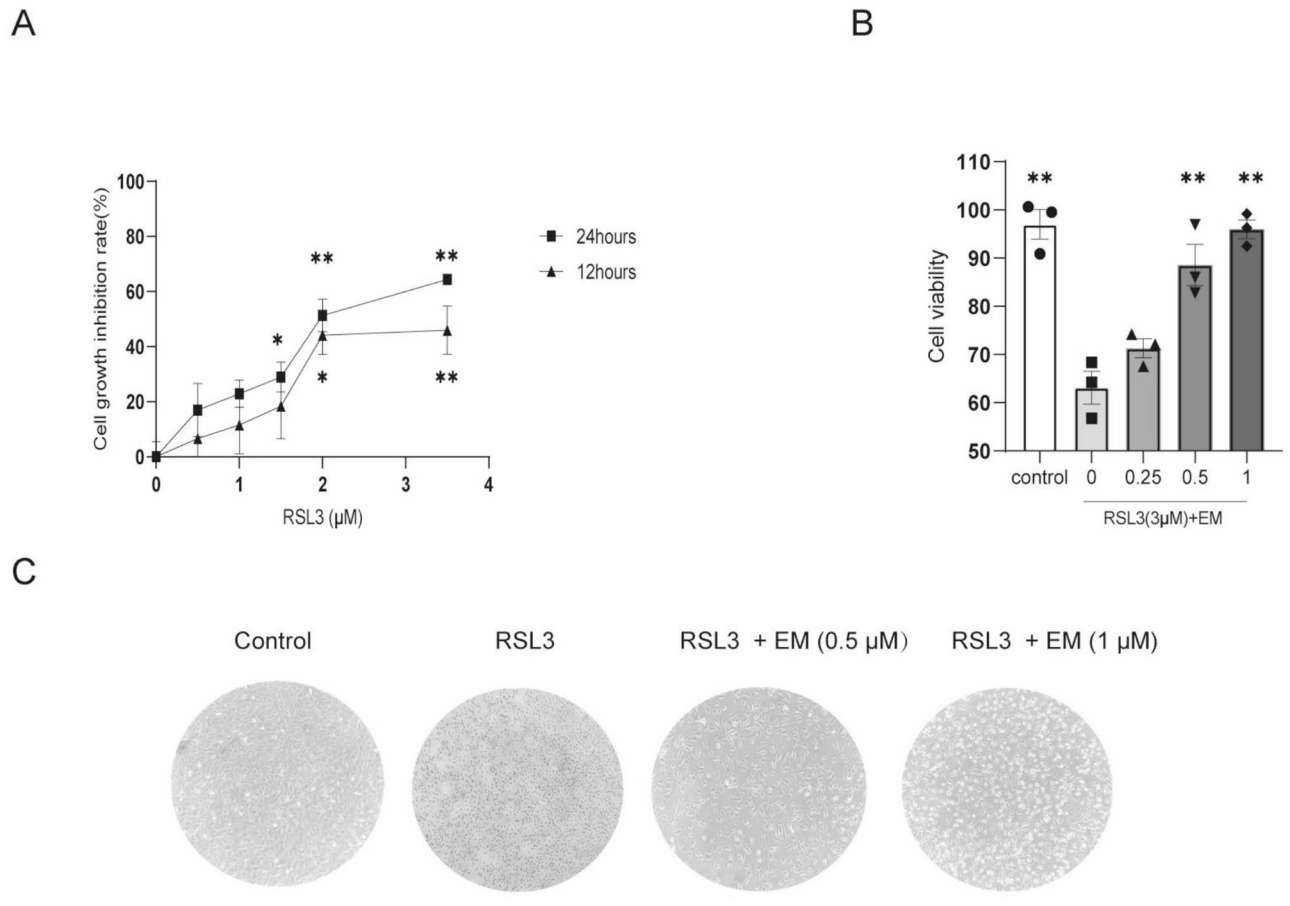

Fig. 1 EMPA reduces the cytotoxicity induced by RSL3 on the EA.hy926 cells. (**A**) The EA.hy926 cell growth inhibition were detected by CCK-8 assay kit after being treated with RSL3. (**B**) The EA.hy926 cell viability were detected by CCK-8 assay kit after being treated with defined concentration of RSL3 and the range of 0.25, 0.5 and 1 μM concentrations of EMPA. (**C**) The morphology of EA.hy926 cells were observed by inverted microscope. *$P < 0.05$ and **$P < 0.01$ vs. RSL3 (0 μM) or RSL3 (3 μM). $n = 3$ biological replicates

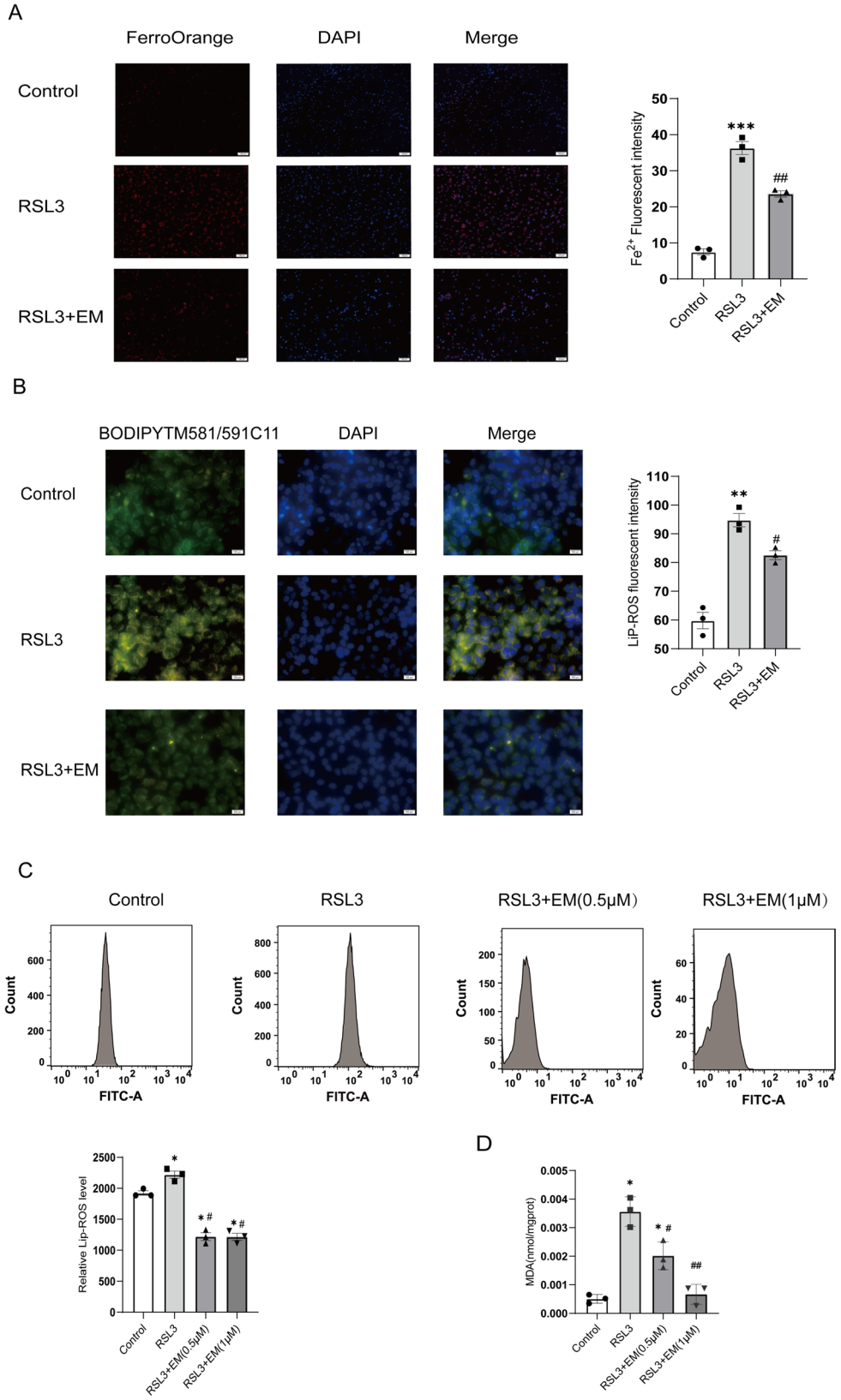

Fig. 2 The effect of EMPA on iron induced lipid peroxidation in EA.hy926 cells. (**A**) The fluorogram of intracellular iron, scale bar of which is 100 μm and quantification were shown in the right panel. (**B**) The fluorogram of intracellular lipid peroxidation, scale bar of which is 100 μm and quantification were shown in the right panel. (**C**) The flow cytograms demonstrated the intracellular peroxidation. (**D**) The histogram demonstrated the content of MDA. $^{*}P<0.05$, $^{**}P<0.01$ and $^{***}P<0.001$ vs. Control group; $^{\#}P<0.05$ and $^{\#\#}P<0.01$ vs. RSL3 group. $n=3$ biological replicates

an intervention could alleviate intracellular iron-dependent peroxidation environment.

EMPA regulates the expression of mRNA and protein of ferroptosis in EA.hy926 cells. It was further to explored whether the EMPA affects the expression of mRNA or protein expression associated with ferroptosis. As compared with the control group, the mRNA of oxidation-related gene ACSL4 was highly expressed in the RSL3-treated group, while the mRNA expression level of cellular antioxidant genes GPX4 was decreased. Following EMPA treatment, the mRNA expression of ACSL4 was markedly decreased, and the mRNA expression of SLC7A11 and GPX4 were increased, particularly at an EMPA concentration of 1 μM concentration (Fig. 3A-C). Western blotting results showed that there was no statistically significant difference in the changes of ACSL4 and SLC7A11 protein, but the protein expression of GPX4 was markedly decreased in the RSL3 group compared with the control group. The protein expression of ACSL4 was decreased following exposure to EMPA intervention, and the expression of GPX4 was significantly increased following treatment with 1 μM EMPA. However, the effect of increasing SLC7A11 protein expression was not significant (Fig. 3D).

EMPA inhibits RSL3 induced ferroptosis by activating the NRF2/HO-1 axis in EA.hy926 cells. Western blotting results showed that, as compared with the control group, there was no significant change in NRF2 and HO-1 protein expression in the RSL3-treated group (both of them were in a low expression) and there was no statistically significant difference. But in the EMPA intervention group, the level of NRF2 and HO-1 expression was elevated, particularly at an EMPA concentration of 1 μM (Fig. 4A).

EA.hy926 cells were further transfected with si-NRF2 to measure the HO-1 and GPX4 protein expression. According to the PCR results of transfection efficiency concerning four types of si-NRF2 the manufacturer provided, the si-NRF2-2 was more suitable for transfection of the EA.hy926 cells, rather than others cells (Fig. S1). The following results showed that the expression levels of HO-1 and GPX4 protein were significantly decreased in the three groups: si-NRF2, si-NC + RSL3 and si-NRF2 + RSL3 groups compared with the NC group (Fig. 4B). These effects could be reversed

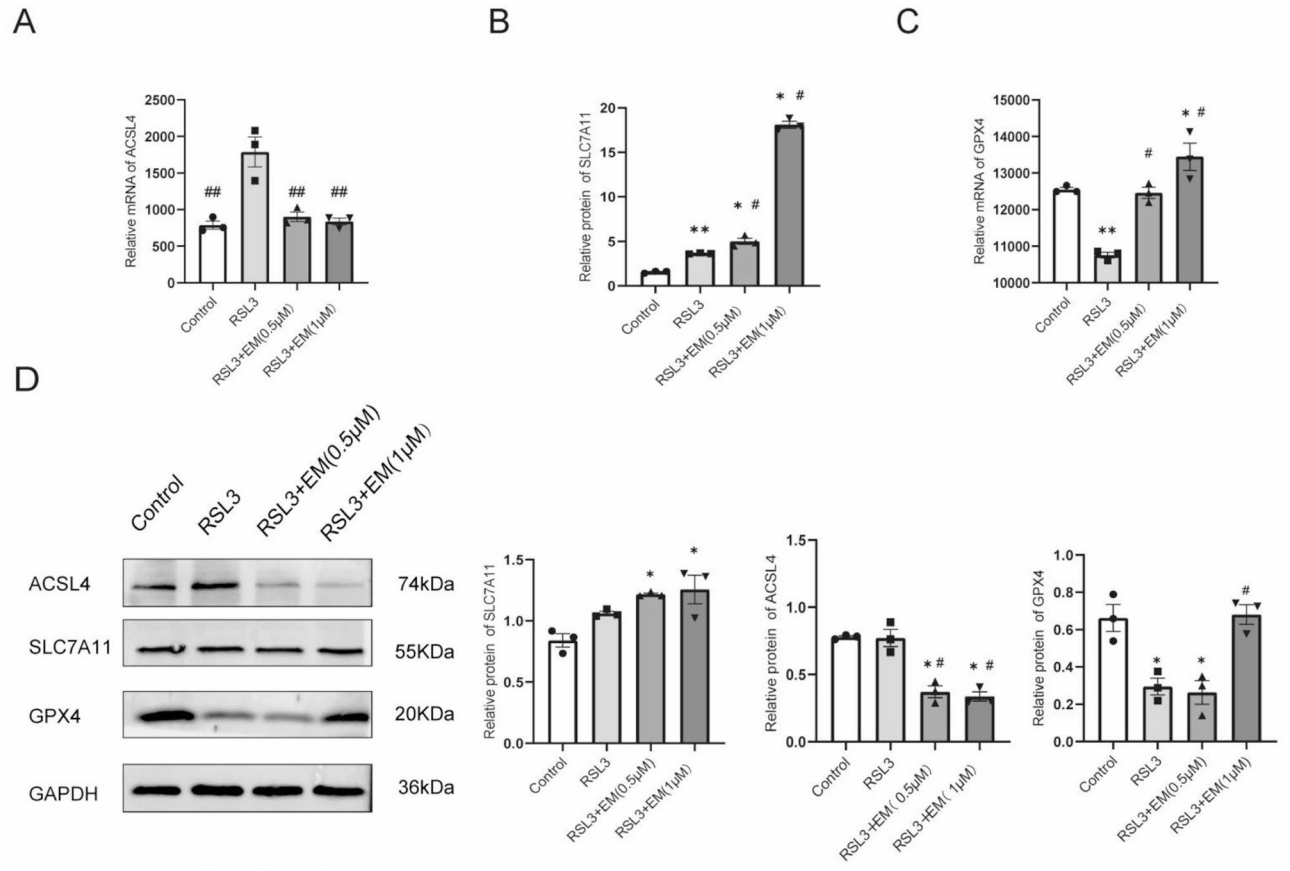

Fig. 3 EMPA regulates the expression of mRNA and protein related to ferroptosis in EA.hy926 cells. (**A**) The mRNA expression of ACSL4. (**B**) The mRNA expression of SLC7A11. (**C**) The mRNA expression of GPX4. (**D**) The protein level of SLC7A11, ACSL4 and GPX4 were measured by western blot with grey value of expression followed. *$P < 0.05$ and **$P < 0.01$ vs.Control group;$^{\#}P < 0.05$ and $^{\#\#}P < 0.01$ vs. RSL3 group. $n = 3$ biological replicates

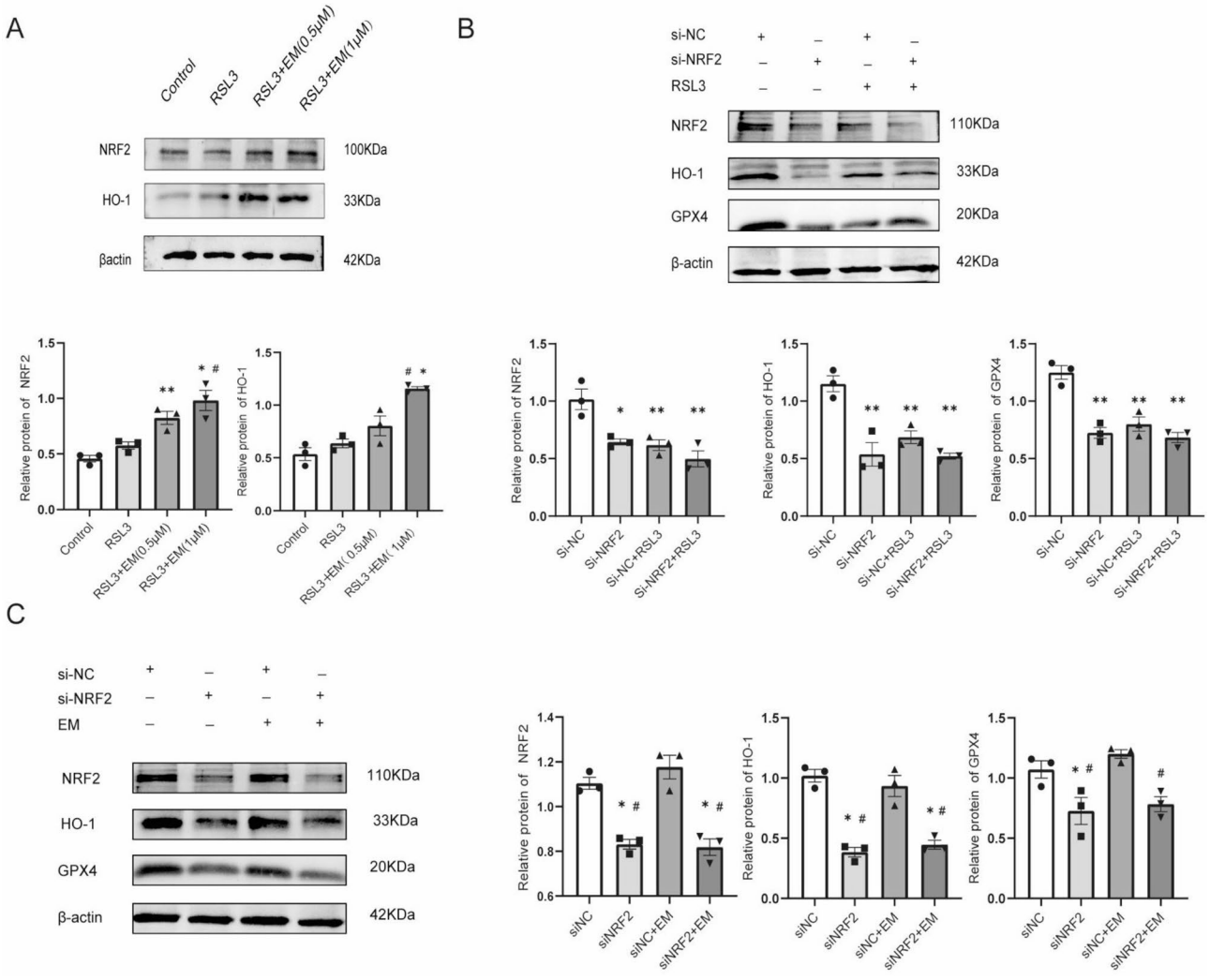

Fig. 4 EMPA inhibits RSL3 induced ferroptosis by activating NRF2/HO-1 axis in EA.hy926 cells. (**A**) The expression of NRF2 and HO-1 were measured by western blot. (**B**) After being transfected with si-NRF2 and dealing with RSL3, the expression of NRF2, HO-1 and GPX4 were measured by western blot. (**C**) After being transfected with si-NRF2 and dealing with EMPA, the expression of NRF2, HO-1 and GPX4 were measured by western blot. *$P < 0.05$, **$P < 0.01$ and ***$P < 0.001$ vs. Control group or siNC; $^{\#}P < 0.05$ and $^{\#\#}P < 0.01$ vs. RSL3 group or siNC + EM. $n = 3$ biological replicates

in the si-NC + EMPA treatment group, but in the si-NRF2 + EMPA group, the expression of HO-1 and GPX4 protein were in a low expression (Fig. 4C).

Discussion

ASCVD is characterized by endothelial dysfunction. Recent evidence suggests that ferroptosis inhibition protects endothelial cells [6]. SGLT2i exert cardiovascular benefits beyond glycemic control [16, 17]. However, the potential mechanism of SGLT2i EMPA protecting endothelial cells remains to be investigated. This study demonstrated that EMPA may inhibit RSL3-induced ferroptosis in EA.hy926 cells by activating the NRF2/HO-1 pathway.

Iron-dependent oxidant reactions have been shown to participate in the whole process of ferroptosis, which contains Fe^{2+}, lipid peroxidation and lipid metabolites [3]. Numerous inducers have been used in recent studies to cause endothelial cell ferroptosis. Shi et al. [18] investigated that homocysteine (Hcy) could induce ferroptosis in endothelial cells and found that intracellular Fe^{2+}, lipid peroxidation, and MDA was increased after the action of Hcy on human umbilical vein endothelial cells EA.hy926. In addition, Bai et al. [6] found that intracellular levels of ROS and the lipid peroxidation product, MDA, were elevated in an ox-LDL-induced mouse aortic endothelial cell injury model. The kirsten rat sarcoma viral oncogene homolog mutant colorectal cancer cell lines were undergoing similar levels of RSL3-induced oxidative stress [19]. In the present study, human umbilical vein endothelial cells EA.hy926 were stimulated with different concentrations (0.5, 1, 1.5, 2 and 3.5 μM) of RSL3 for 12 and 24 h. It was observed that cellular activity

decreased with the increasing concentration of RSL3 and the duration of its action. Furthermore, the intracellular Fe^{2+} levels, lipid peroxide levels and MDA levels were significantly increased following RSL3 treatment. Fe^{2+} serves as a catalytic substrate in the Fenton reaction, while MDA and lipid peroxidation products are downstream markers of this process [20]. These findings suggested that RSL3 may activate Fenton reaction to drive lipid peroxidation, leading to ferroptosis. Therefore, the induction of ferroptosis in EA.hy926 cells by RSL3 in this study has provided a validated experimental model in subsequent experiments. Increasing studies have shown that SGLT2i can protect diabetic disease from ferroptosis [21]. EMPA attenuates cardiotoxicity through the suppression of ferroptosis [22]. However, whether EMPA could protect endothelial cells from ferroptosis was not investigated. The results of the present study suggested that endothelial cell activity was increased and intracellular Fe^{2+}, lipid peroxides and MDA levels were decreased in the EMPA intervention group, as compared with the RSL3 treatment group. The preliminary results demonstrated that EMPA could reduce the unstable Fe^{2+} content of EA.hy926 human umbilical vein endothelial cells and attenuate lipid peroxidation damage.

Genes including GPX4, SLC7A11, and ACSL4 are key regulators of ferroptosis. Sui et al. [23] showed that, following the treatment of colon cancer cells with RSL3, the intracellular levels of ROS and transferrin were increased, and the expression of GPX4 was decreased, which could be alleviated by overexpressing GPX4. Merkel et al. [24] reported that the overexpression of ACSL4 increased the sensitivity of human embryonic kidney cells to the effects of RSL3 and led to ferroptosis and RSL3-induced oxidative damage. In the present study, intracellular GPX4 expression was decreased and ACSL4 expression was increased following RSL3 treatment, while the expression of SLC7A11 was not significantly affected, as previous studies showing that ferroptosis inducers such as erastin, sulfasalazine, and sorafenib could suppresse SLC7A11 activity, thereby inhibiting cystine uptake and glutathione biosynthesis, while RSL3 induces ferroptosis through a distinct mechanism involving direct GPX4 inactivation rather than SLC7A11 inhibition [25]. The mRNA and protein expression levels of intracellular GPX4 increased and those of ACSL4 decreased in a concentration-dependent manner following treatment with different concentrations of EMPA. The above results also suggested that EMPA could regulate genes associated with ferroptosis.

NRF2, as a transcription factor, activates the expression of protective genes for iron metabolism, oxidative defense and redox signaling during ferroptosis [3]. Cai et al. [26] showed that astaxanthin attenuates acetaminophen-induced ferroptosis by increasing GPX4 expression through the activation of the NRF2/HO-1 pathway. Qi et al. [27] demonstrated that quercetin inhibits ferroptosis in renal tubular epithelial cells by increasing the expression of transferrin receptor protein and GPX4 through the activation of the NRF2/HO-1 signaling pathway. Gao et al. [28] showed that annexin A5 alleviates traumatic brain injury induced ferroptosis and oxidative stress damage through Nrf2/HO-1 pathway. It was suggested that the increased protein expression of NRF2/HO-1 pathway can play a role in inhibiting ferroptosis. However, whether EMPA could resist endothelial cell ferroptosis through the NRF2/HO-1 pathway remains unknown. In the present study, the NRF2 and HO-1 protein expression levels were significantly elevated in concentration-dependent manner in the EMPA intervention group compared to the RSL3-treated group. These results were significantly reversed following siNRF2 transfection. The target genes HO-1 and GPX4 were lowly expressed as the siNRF2 transfected cells, which was further suggested that EMPA may alleviate RSL3-induced ferroptosis in human umbilical vein endothelial cells EA.hy926 by activating the NRF2/HO-1 pathway.

The findings provided in the present study can help refine the treatment of endothelial cell dysfunction. But there are still some limitations in this study. Merely quantifying intracellular Fe^{2+} levels and lipid peroxidation markers are insufficient to conclusively demonstrate that RSL3 accelerates Fenton reaction. In addition, the Fenton reaction was further verified using hydroxyl free radical specific fluorescence probes (such as HPF or APF) combined with flowcytometry or fluorescence microscopy observation or electron paramagnetic resonance (EPR) technology to directly detect free radical signals [29]. Although the EA.hy926 cell line has been extensively utilized in atherosclerosis-related studies owing to exhibiting infinite proliferative capacity, experimental tractability, and high culture stability, the cell lines may incompletely recapitulate the dynamic functional adaptations of native endothelia within atherosclerotic microenvironments [30, 31]. Future in vivo investigations are required to confirm the effect of EMPA on inhibition of ferroptosis in endothelial cells.

Conclusions

This study demonstrates a novel mechanism that the SGLT2i EMPA inhibits endothelial cells ferroptosis by activation the NRF2/HO-1 signaling pathway. In the RSL3-induced EA.hy926 cell model, EMPA significantly reduced content of intracellular Fe^{2+} levels, lipid peroxidation and MDA, as well as up-regulate the expression of the antioxidant enzyme GPX4 and inhibit the iron death-promoting factor ACSL4. Furthermore, EMPA enhances cellular oxidative stress defense through activation of the NRF2/HO-1 axis, while NRF2 gene silencing completely reverses its protective effect. Our findings expand

pharmacological profile of EMPA beyond glycemic control, positioning it as a promising cardio-protective agent through ferroptosis suppression.

Supplementary Information

The online version contains supplementary material available at https://doi.org/10.1186/s12872-025-04890-7.

Supplementary Material 1

Supplementary Material 2

Acknowledgements
We would like to thank all of members of Cardiovascular Research Center for scientific discussion and technical support.

Author contributions
Z.S.Y as the corresponding of the article provided the design at the study. W.Z.L and L.S.M performed experiments and analyzed data.S.J.H, C.D, and L.S.L provided technical support and instruction. W.Z.L wrote the paper and drafted graphs. Y.S.Q, Y.K.J, Z.W, G.X and L.S.X helped to modify and revise article.

Funding
This study was supported by interdisciplinary project of Dalian University (DLUXK-2024-QN-016).

Data availability
The authors declare that the data supporting the findings of this study are available within the paper and its Supplementary Information files. Should any raw data files be needed in another format they are available from the corresponding author upon reasonable request.

Declarations

Ethics approval and consent to participate
Not applicable.

Consent for publication
The results/data/figures in this manuscript have not been published elsewhere, nor are they under consideration by another publisher.

Competing interests
The authors declare that there is no competing financial interest that influences teamwork and personal relationships.

Clinical trial number
Not applicable.

Received: 10 January 2025 / Accepted: 26 May 2025
Published online: 07 June 2025

References

1. Gimbrone MA Jr., García-Cardeña G. Endothelial cell dysfunction and the pathobiology of atherosclerosis. Circ Res. 2016;118(4):620–36.
2. Xu S, Ilyas I, Little PJ, Li H, Kamato D, Zheng X, Luo S, Li Z, Liu P, Han J, et al. Endothelial dysfunction in atherosclerotic cardiovascular diseases and beyond: from mechanism to pharmacotherapies. Pharmacol Rev. 2021;73(3):924–67.
3. Tang D, Chen X, Kang R, Kroemer G. Ferroptosis: molecular mechanisms and health implications. Cell Res. 2021;31(2):107–25.
4. Wang Y, Zhao Y, Ye T, Yang L, Shen Y, Li H. Ferroptosis signaling and regulators in atherosclerosis. Front Cell Dev Biol. 2021;9:809457.
5. Lee J, Roh JL. SLC7A11 as a gateway of metabolic perturbation and ferroptosis vulnerability in Cancer. Antioxid (Basel) 2022, 11(12).
6. Bai T, Li M, Liu Y, Qiao Z, Wang Z. Inhibition of ferroptosis alleviates atherosclerosis through attenuating lipid peroxidation and endothelial dysfunction in mouse aortic endothelial cell. Free Radic Biol Med. 2020;160:92–102.
7. Wang X, Zhang M, Mao C, Zhang C, Ma W, Tang J, Xiang D, Qi X. Icariin alleviates ferroptosis-related atherosclerosis by promoting autophagy in xo-LDL-induced vascular endothelial cell injury and atherosclerotic mice. Phytother Res. 2023;37(9):3951–63.
8. Aguiar C, Duarte R, Carvalho D. New approach to diabetes care: from blood glucose to cardiovascular disease. Rev Port Cardiol (Engl Ed). 2019;38(1):53–63.
9. Cai C, Guo Z, Chang X, Li Z, Wu F, He J, Cao T, Wang K, Shi N, Zhou H, et al. Empagliflozin attenuates cardiac microvascular ischemia/reperfusion through activating the AMPKα1/ULK1/FUNDC1/mitophagy pathway. Redox Biol. 2022;52:102288.
10. Zou R, Shi W, Qiu J, Zhou N, Du N, Zhou H, Chen X, Ma L. Empagliflozin attenuates cardiac microvascular ischemia/reperfusion injury through improving mitochondrial homeostasis. Cardiovasc Diabetol. 2022;21(1):106.
11. Kolijn D, Pabel S, Tian Y, Lódi M, Herwig M, Carrizzo A, Zhazykbayeva S, Kovács Á, Fülöp G, Falcão-Pires I, et al. Empagliflozin improves endothelial and cardiomyocyte function in human heart failure with preserved ejection fraction via reduced pro-inflammatory-oxidative pathways and protein kinase Gα oxidation. Cardiovasc Res. 2021;117(2):495–507.
12. Li X, Wang M, Kalina JO, Preckel B, Hollmann MW, Albrecht M, Zuurbier CJ, Weber NC. Empagliflozin prevents oxidative stress in human coronary artery endothelial cells via the NHE/PKC/NOX axis. Redox Biol. 2024;69:102979.
13. Loboda A, Damulewicz M, Pyza E, Jozkowicz A, Dulak J. Role of Nrf2/HO-1 system in development, oxidative stress response and diseases: an evolutionarily conserved mechanism. Cell Mol Life Sci. 2016;73(17):3221–47.
14. Yan R, Lin B, Jin W, Tang L, Hu S, Cai R. NRF2, a superstar of ferroptosis. Antioxid (Basel) 2023, 12(9).
15. Zhang Q, Yao M, Qi J, Song R, Wang L, Li J, Zhou X, Chang D, Huang Q, Li L, et al. Puerarin inhibited oxidative stress and alleviated cerebral ischemia-reperfusion injury through PI3K/Akt/Nrf2 signaling pathway. Front Pharmacol. 2023;14:1134380.
16. Liu Z, Ma X, Ilyas I, Zheng X, Luo S, Little PJ, Kamato D, Sahebkar A, Wu W, Weng J, et al. Impact of sodium glucose cotransporter 2 (SGLT2) inhibitors on atherosclerosis: from Pharmacology to pre-clinical and clinical therapeutics. Theranostics. 2021;11(9):4502–15.
17. Vallon V, Verma S. Effects of SGLT2 inhibitors on kidney and cardiovascular function. Annu Rev Physiol. 2021;83:503–28.
18. Shi J, Chen D, Wang Z, Li S, Zhang S. Homocysteine induces ferroptosis in endothelial cells through the systemXc(-)/GPX4 signaling pathway. BMC Cardiovasc Disord. 2023;23(1):316.
19. Yang J, Mo J, Dai J, Ye C, Cen W, Zheng X, Jiang L, Ye L. Cetuximab promotes RSL3-induced ferroptosis by suppressing the Nrf2/HO-1 signalling pathway in KRAS mutant colorectal cancer. Cell Death Dis. 2021;12(11):1079.
20. Mortensen MS, Ruiz J, Watts JL. Polyunsaturated fatty acids drive lipid peroxidation during ferroptosis. Cells 2023, 12(5).
21. Lu Q, Yang L, Xiao JJ, Liu Q, Ni L, Hu JW, Yu H, Wu X, Zhang BF. Empagliflozin attenuates the renal tubular ferroptosis in diabetic kidney disease through AMPK/NRF2 pathway. Free Radic Biol Med. 2023;195:89–102.
22. Min J, Wu L, Liu Y, Song G, Deng Q, Jin W, Yu W, Abudureyimu M, Pei Z, Ren J. Empagliflozin attenuates trastuzumab-induced cardiotoxicity through suppression of DNA damage and ferroptosis. Life Sci. 2023;312:121207.
23. Sui X, Zhang R, Liu S, Duan T, Zhai L, Zhang M, Han X, Xiang Y, Huang X, Lin H, et al. RSL3 drives ferroptosis through GPX4 inactivation and ROS production in colorectal Cancer. Front Pharmacol. 2018;9:1371.
24. Merkel M, Goebel B, Boll M, Adhikari A, Maurer V, Steinhilber D, Culmsee C. Mitochondrial reactive oxygen species formation determines ACSL4/LPCAT2-Mediated ferroptosis. Antioxid (Basel) 2023, 12(8).
25. Song X, Zhu S, Chen P, Hou W, Wen Q, Liu J, Xie Y, Liu J, Klionsky DJ, Kroemer G, et al. AMPK-Mediated BECN1 phosphorylation promotes ferroptosis by directly blocking system X(c)(-) activity. Curr Biol. 2018;28(15):2388–e23992385.
26. Cai X, Hua S, Deng J, Du Z, Zhang D, Liu Z, Khan NU, Zhou M, Chen Z. Astaxanthin activated the Nrf2/HO-1 pathway to enhance autophagy and inhibit ferroptosis, ameliorating Acetaminophen-Induced liver injury. ACS Appl Mater Interfaces. 2022;14(38):42887–903.
27. Feng Q, Yang Y, Qiao Y, Zheng Y, Yu X, Liu F, Wang H, Zheng B, Pan S, Ren K, et al. Quercetin ameliorates diabetic kidney injury by inhibiting ferroptosis via activating Nrf2/HO-1 signaling pathway. Am J Chin Med. 2023;51(4):997–1018.

28. Gao Y, Zhang H, Wang J, Li F, Li X, Li T, Wang C, Li L, Peng R, Liu L, et al. Annexin A5 ameliorates traumatic brain injury-induced neuroinflammation and neuronal ferroptosis by modulating the NF-κB/HMGB1 and Nrf2/HO-1 pathways. Int Immunopharmacol. 2023;114:109619.
29. Peng S, Chen G, Yu KN, Feng Y, Zhao L, Yang M, Cao W, Almahi WAA, Sun M, Xu Y, et al. Synergism of non-thermal plasma and low concentration RSL3 triggers ferroptosis via promoting xCT lysosomal degradation through ROS/AMPK/mTOR axis in lung cancer cells. Cell Commun Signal. 2024;22(1):112.
30. Bouïs D, Hospers GA, Meijer C, Molema G, Mulder NH. Endothelium in vitro: a review of human vascular endothelial cell lines for blood vessel-related research. Angiogenesis. 2001;4(2):91–102.
31. Wang D, Chen Z, Wai Kan Yeyng A, Atanasov AG. Differences between common endothelial cell models (primary human aortic endothelial cells and EA.hy926 cells) revealed through transcriptomics, bioinformatics, and functional analysis. Curr Res Biotechnol. 2021;3:135–45.

Publisher's note